NIMA-related kinase *Tb*NRKC is involved in basal body separation in *Trypanosoma brucei*

Lydie C. Pradel, Mélanie Bonhivers, Nicolas Landrein and Derrick R. Robinson*

Laboratoire de Génomique Fonctionnelle des Trypanosomatides, CNRS UMR 5162, Université Bordeaux 2, 146 rue Léo Saignat, Bât. 3A, 33076 Bordeaux CEDEX, France

*Author for correspondence (e-mail: Derrick.Robinson@parasitmol.u-bordeaux2.fr)

Accepted 20 January 2006
Journal of Cell Science 119, 1852-1863 Published by The Company of Biologists 2006
doi:10.1242/jcs.02900

Summary

The NIMA-related kinase 2 (NEK 2) has important cell cycle functions related to centriole integrity and splitting. *Trypanosoma brucei* does not possess centrioles, however, cytokinesis is coupled to basal body separation events. Here we report the first functional characterisation of a *T. brucei* basal body-cytoskeletal NIMA-related kinase (NRK) protein, *Tb*NRKC. The *Tb*NRKC kinase domain has high amino acid identity with the human NEK1 kinase domain (50%) but also shares 42% identity with human NEK2. *Tb*NRKC is expressed in bloodstream and procyclic cells and functions as a bona fide kinase in vitro. Remarkably, RNAi knockdown of *TbNRKC* and overexpression of kinase-dead *Tb*NRKC in procyclic forms induces the accumulation of cells with four basal bodies, whereas overexpression of active protein produces supernumary basal bodies and blocks cytokinesis. *Tb*NRKC is located on mature and immature basal bodies and is the first *T. brucei* NRK to be found associated with the basal body cytokinesis pathway.

Key words: NEK, Basal body, Cytokinesis, *T. brucei,* Cell cycle

Introduction

The never in mitosis gene A (NIMA)-related kinases (NEKs) belong to a family of ubiquitous serine/threonine kinases that promote cell cycle events and have been implicated in driving G2-M progression (Fry, 2002; Fry et al., 1998a; Fry et al., 1998b; Rhee and Wolgemuth, 1997). Members of this family are also implicated in polycystic kidney diseases (PKD) (Liu et al., 2002; Mahjoub et al., 2002; Mahjoub et al., 2004). Although NEKs are the most closely related kinases to NIMA they serve different functions. Mammalian NEK1 is highly expressed in meiotic germ cells and is considered to have a role in controlling meiotic events (Letwin et al., 1992); it is also one of the key proteins involved in PKD (Upadhya et al., 2000) and recovery from DNA damage (Polci et al., 2004). Mammalian NEK2 is one of the most characterised of the NEKs and has, across the catalytic kinase domain, 44% amino acid identity with NIMA. The splice variant NEK2A is enriched at the centrosome and functional studies in homologues of NEK2 in mammalian and *Xenopus* cells suggest a role in centrosome maintenance, structure and centriole splitting (Fry et al., 2000; Fry et al., 1998a; Fry et al., 1998b; Hames et al., 2001; Twomey et al., 2004). The first non-vertebrate orthologue of human NEK2 (*Hs*NEK2) was identified in *Dictyostelium discoidium* (*Dd*Nek2). *Dd*Nek2 shares 43% overall amino acid identity with *Hs*NEK2 and 54% identity within the catalytic domain. Overexpression of *Dd*Nek2 stimulates the formation of supernumerary asters and microtubule organising centres (MTOCs) (Graf, 2002).

Trypanosoma brucei is protozoan parasite responsible for sleeping sickness in humans and Nagana in animals (Chappuis et al., 2005; Kioy et al., 2004; Vickerman, 1985). The *T. brucei* procyclic insect form coordinates the replication and segregation of its single-copy organelles: the nucleus, mitochondria (including its genome, the kinetoplast) and flagellum. Wild-type G1 cells have a mature basal body that forms a flagellum and an immature basal body, which has not yet formed its own flagellum. As the cell passes through the cell cycle, the immature basal body matures and initiates the growth of a new flagellum. This is then accompanied by the formation of two immature basal bodies. Consequently, immature basal bodies are always very closely physically associated with a mature basal body and hence a flagellum (Sherwin and Gull, 1989). Basal bodies are also physically linked to each other in G1 of the cell cycle and are always physically linked to the kinetoplast by proteins that have yet to be identified (Ogbadoyi et al., 2003; Robinson and Gull, 1991). To date the only cytoskeletal cell cycle marker related to the control of cytokinesis in trypanosomes is the separation of its basal bodies. If basal body separation is blocked, the cell does not undergo cytokinesis (Ploubidou et al., 1999).

Although the roles of NEK proteins have been studied in mammals, *Xenopus* and *Drosophila*, little is known about the mechanistic basis for these phenomena in protists. Previous searches for *T. brucei* NIMA-related kinases (NRKs) resulted in the identification two kinase genes, namely NRKA and B. They have highest expression levels and activity in bloodstream form, G0-arrested, stumpy cells and are considered to be involved in parasite differentiation (Gale et al., 1994; Gale and Parsons, 1993). The location of these proteins within the cell is unknown. In this study we have identified the first *T. brucei* basal body NRK protein, which we have named *Tb*NRKC. NRKA and NRKB have high amino acid identity with the N-terminus of *Tb*NRKC (~37% identity).

We show that *Tb*NRKC can control the passage of procyclic cells through the cell cycle and that recombinant *Tb*NRKC has kinase activity in vitro. RNAi knockdown of *TbNRKC* and overexpression of kinase-dead *Tb*NRKC in procyclic forms increases the proportion of cells with four basal bodies. RNAi knockdown (and kinase-dead *Tb*NRKC overexpression) also produces a minor population of cells that do not separate their basal bodies. Overexpression of TY1-tagged *Tb*NRKC or native protein in procyclic cells produces multinucleated cells with enlarged kinetoplasts and abnormally high numbers of non-flagellated, non-separated basal bodies. These data suggest that *Tb*NRKC is involved in controlling basal body separation and thus cytokinesis.

Results

*Tb*NRKC is a NIMA-related kinase of *T. brucei*

Two NIMA-related kinases have been previously identified in *T. brucei*, *Tb*NRKA and *Tb*NRKB. We used human *Hs*Nek2 and *Aspergillus nidulans* NIMA protein sequences to search for additional putative *Tb*NRK proteins. Both queries gave high amino acid identity scores over the kinase domain (42% and 39% respectively) for a protein encoded by a gene located on chromosome 10 (annotated on GeneDB as Tb10.70.7860). We have named this protein *Tb*NRKC (for *T. brucei* NIMA Related Kinase). *TbNRKC* encodes a protein of 764 amino acids in length, which has a predicted size of 87.2 kDa. The protein contains all 11 conserved sub-domains of the protein

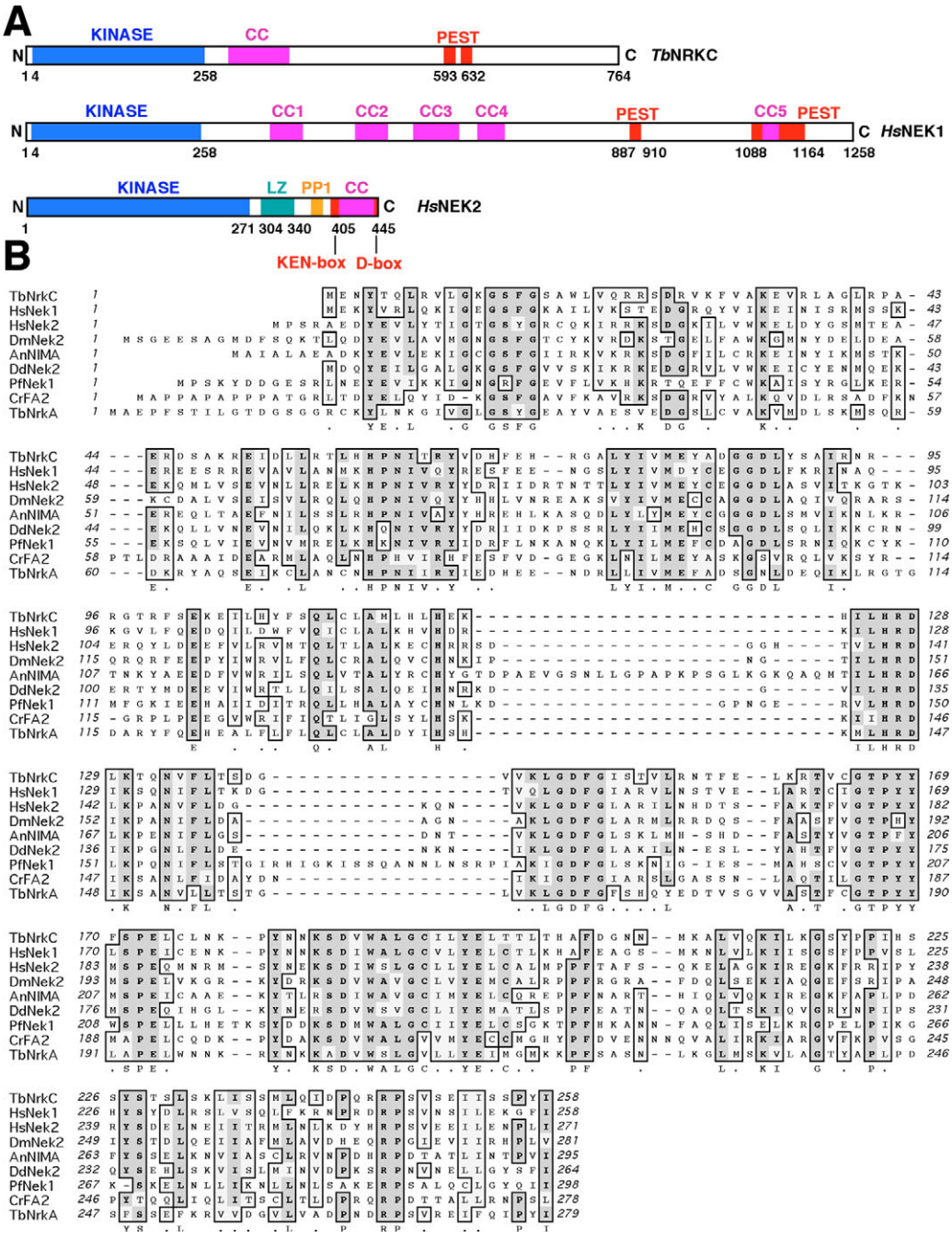

Fig. 1. (A) Schematic representation of *Tb*NRKC, *Hs*NEK1 and *Hs*NEK2 proteins. *Tb*NRKC contains a N-terminus kinase domain, a coiled-coil domain (CC), two PEST motifs, but does not contain a leucine zipper motif (LZ). *Hs*NEK1 contains a N-terminus kinase domain, several coiled-coil domains and two PEST domains but no LZ motif, KEN or D-Box. *Hs*NEK2 contains a coiled-coil domain, a leucine zipper, a KEN-box, a D-box and a phosphatase protein1 binding site (PP1). (B) The kinase domain of *Tb*NRKC is highly conserved in NEKs. Residues conserved in more than 60% of the proteins are dark grey. Similar residues are light grey. Sequences used: *Tb*NRKC (DQ054526), *Hs*Nek1 (Q96PY6), *Hs*Nek2 (P51955), *Dm*Nek2 (NM_132187), *An*NIMA (P11837), *Dd*Nek2 (SLD805), *Pf*Nek1 (CAB76949), *Cr*Fa2 (AAL86904) and *Tb*NrkA (Q08942).

kinase family (Hanks and Hunter, 1995; Hanks and Quinn, 1991). These include: (1) The glycine loop Gly11-x-Gly13-x-x-Gly16, which forms a portion of the ATP-binding region; (2) The catalytic loop Arg127-Asp128-x-x-x-x-Asn133, which is involved in catalytic activity and in guiding the peptide substrate into the correct orientation; (3) The Glu173, Asp185 and Arg246 residues, which are involved in the stabilisation of the protein. The catalytic domain of *Tb*NRKC is similar to other NEKs in general structural arrangement (Fig. 1A,B).

The catalytic domain of *Tb*NRKC has a high identity with that of *Hs*NEK1 (50%) and shares 42% of identity and similar domains with human *Hs*NEK2. *Hs*NEK1, *Hs*NEK2 and *Tb*NRKC have coiled-coil and degradation domains (O'Connell et al., 2003). *Tb*NRKC has two PEST sequences commonly found in protein targeted for rapid degradation (Rechsteiner and Rogers, 1996). This domain is found in most NEKs including, *Hs*NEK1, NIMA, NIM-1 of *Neurospora crassa*, FIN1p of *Schizosaccharomyces pombe* and most human NEKs (O'Connell et al., 2003). *Hs*NEK2 has similar targeting domains known as the KEN and D-Boxes (Fig. 1A).

*Tb*NRKC is a functional kinase in vitro

To test whether *Tb*NRKC functions as a kinase, we expressed and purified *Tb*NRKC protein using metal chelate chromatography. The recombinant protein (NRKC-6His, calculated size of 88.2 kDa) was tested using a standard kinase assay. Purified recombinant protein was able to phosphorylate a α/β casein substrate in vitro. Furthermore, NRKC-6His appeared to be selective for β casein, which was highly phosphorylated compared with α casein (Fig. 2A, lane 2 arrowhead). NRKC-6His did not phosphorylate BSA, which is the negative control substrate. To ensure that the kinase activity was due to *Tb*NRKC protein and not bacterial contamination, the Lys33 of the putative kinase domain (which is conserved in all NEK kinase domains) was mutated to methionine. The resulting mutated protein (mNRKC-6His) had no kinase activity (Fig. 2A, lanes 6-8). The corresponding Coomassie-Blue-stained gel (Fig. 2B) and western blot (Fig. 2C), were used as loading controls. From this data we conclude that *Tb*NRKC is a bona fide kinase and that the Lys33 is essential for kinase activity.

*Tb*NRKC is a basal body protein

Trypanosomes do not have centrioles (Ogbadoyi et al., 2000). However, G1 trypanosomes have a pair of basal bodies, a mature basal body, which is the origin of the axoneme and an immature basal body that will form the new flagellum. These basal bodies are not involved in spindle formation (Ogbadoyi et al., 2000; Ploubidou et al., 1999; Vickerman et al., 1988). As *Hs*NEK2 protein has been localised in the centrioles we sought to identify the cellular localisation of *Tb*NRKC. We cloned the non-conserved, non-kinase, domain (i.e. the terminal 494 residues) of *Tb*NRKC and used its *E. coli*-expressed protein to produce the mouse polyclonal anti-serum (Isa-1).

Western blotting studies indicated that Isa-1 recognises a protein band of apparent relative mass of ~90 kDa from whole-cell preparations of wild-type procyclic and bloodstream cells. This band is similar to the calculated mass (87.2 kDa) of *Tb*NRKC protein (Fig. 3A, lanes 3 and 4). To ensure that Isa-1 is specific for recombinant NRKC-6HIS protein and

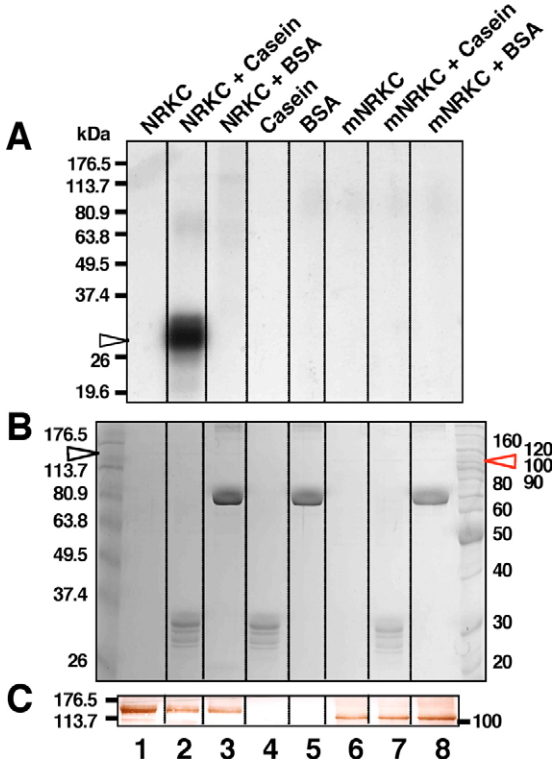

Fig. 2. (A) Purified recombinant *Tb*NRKC-6His protein (NRKC, black left arrowhead) phosphorylates α/β casein substrate in vitro and preferentially phosphorylates β casein (lane 2 arrowhead). The negative control BSA (apparent molecular mass 67 kDa) is not phosphorylated (lane 3). Purified kinase-dead *Tb*NRKC-6His protein (mNRKC) (red arrowhead) does not phosphorylate the α/β casein (lane 7) or BSA (lane 8). Controls: lane 1 *Tb*NRKC alone, lane 4 α/β casein alone, lane 5 BSA alone, lane 6 mNRKC alone. (B) Corresponding Coomassie-Blue-stained SDS-PAGE as protein loading control. (C) Corresponding western blot with Isa-1 polyclonal antibody as recombinant protein loading control. Pre-stained (left) and non-prestained (right) molecular mass markers show a slight discrepancy in the relative migration in the gel. Note that the recombinant mNRKC protein (B, position indicated by red arrowhead) migrates at a lower molecular mass than the recombinant NRKC (B, position indicated by black arrowhead). Arrowheads indicate where mNRKC and NRKC would normally run on SDS-PAGE.

endogenous *Tb*NRKC protein, the polyclonal antibody was first saturated with the recombinant NRKC-6HIS protein then tested on western blot (Fig. 3B). After saturation, no recombinant or endogenous protein *Tb*NRKC protein was observed by western blot, indicating that Isa-1 is indeed specific for *Tb*NRKC protein. To identify the location of *Tb*NRKC protein, we probed cytoskeletons of procyclic forms with Isa-1 by immunofluorescence. A fluorescence signal was observed on the flagellum basal bodies (Fig. 3C,a-d). This signal was not observed when probed with saturated Isa-1 (Fig. 3C,e-h), but was sometimes accompanied by a weak flagellar attachment zone background signal (Fig. 3C,a-d). We observed basal body signals (and weak transition zone signals) in cells expressing a C-terminal-GFP fusion form of *Tb*NRKC (NRKC-GFP). Thus confirming a basal body location for *Tb*NRKC (Fig. 3C,i-l). Double labelling of cytoskeletons with anti-GFP and YL1/2 (a marker for tyrosinated tubulin, used to

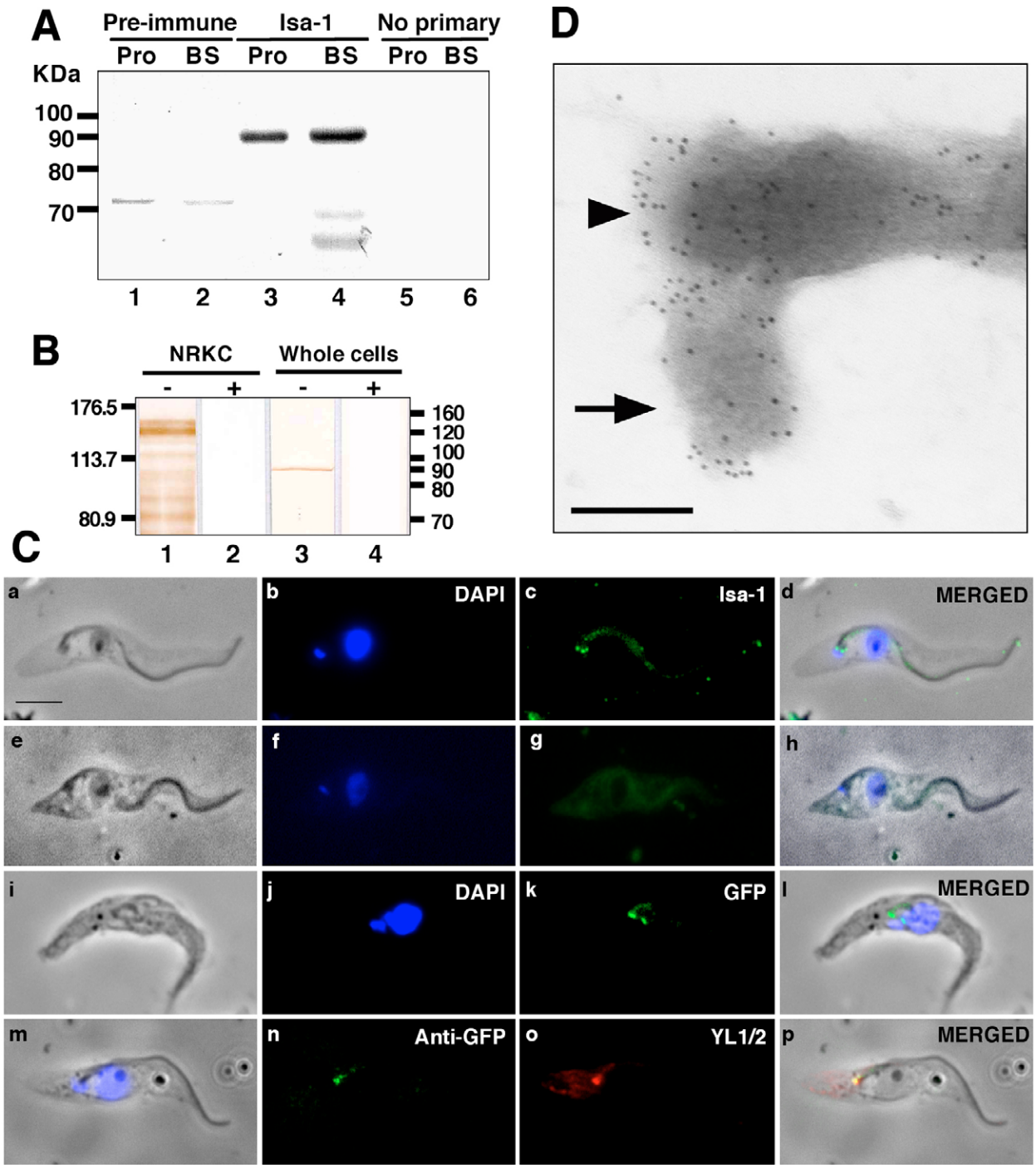

Fig. 3. (A) The polyclonal antibody Isa-1 recognises the ~90 kDa *Tb*NRKC protein, which is expressed in the procyclic (Pro) and bloodstream forms (BS) of *T. brucei* (2.5×10^6 cells/well loaded) on western blot. Controls: pre-immune on procyclic (lane 1) and bloodstream (lane 2) forms, no primary antibody (lanes 5 and 6). (B) The Isa-1 polyclonal antibody specificity to the NRKC protein was tested on western blot of the purified recombinant *Tb*NRKC protein (lanes 1 and 2) and whole cells (lanes 3 and 4) without (–) or with (+) pre-incubation of Isa-1 with the recombinant protein (saturation assay). (C) *Tb*NRKC is a basal body protein. *T. brucei* cytoskeletons (a-d) were prepared for immunofluorescence. A basal body and weak FAZ signals were observed using Isa-1 (c). Isa-1 specificity was assessed by saturation assays (e-h). A tetracycline induced (48 hours) NRKC-GFP expressing cell (i-l) illustrates direct GFP fluorescence on the basal bodies. Cytoskeletons of NRKC-GFP-expressing cells (m-p) probed with anti-GFP antibody (n) and YL-1/2 (o) confirms the basal body location of *Tb*NRKC. a,e,i, phase-contrast images; m, phase-contrast image plus DAPI staining. Bar, 5 μm. (D) Flagella probed with Isa-1 visualised by electron microscopy. The majority of the Isa-1 labelling is on the proximal end of the mature basal body (arrowhead), some label is observed on the transition zone. The Isa-1 labelling of the immature basal body (arrow) cannot be clearly defined as proximal or distal because the immature basal body in vivo is orthogonal to the mature basal body. Some labelling can be observed between the mature and the immature basal bodies. Bar, 250 nm.

identify basal bodies in *T. brucei*) (Kilmartin et al., 1982) confirms that *Tb*NRKC is located to the basal bodies (Fig. 3Cm-p). We probed isolated flagellae with Isa-1 antibody and visualised the labelling by electron microscopy (Fig. 3D). The majority of the Isa-1 labelling is on the proximal end of the mature basal body with some label observed on the transition zone. The Isa-1 labelling of the immature basal body cannot be clearly defined as proximal or distal because the immature basal body in vivo is orthogonal in orientation with respect to the mature basal body and can be randomly re-oriented when placed on the electron microscope grid. However, some labelling can be observed between the mature and the immature basal bodies (Fig. 3D).

RNAi knockdown of *Tb*NRKC is not lethal but induces the accumulation of a four-basal-body phenotype

Isa-1 was used to determine the presence or absence of *Tb*NRKC in RNAi induced cells. We used a 640 bp PCR fragment of the *TbNRKC* gene to make a stem-loop RNAi construct, which was transfected into procyclic EATRO1125-T7T cells. These cells were cloned and used in RNAi studies. No growth difference was observed between induced and non-induced cells after 10 days of induction, indicating that RNAi knockdown of the *Tb*NRKC protein was not lethal over this time period (Fig. 4A). However, induced cells were negative for a basal body signal after 48 hours of induction (Fig. 4B,d,f,h). Western blot data indicated a rapid loss of *Tb*NRKC, which was undetectable 48 hours after induction (Fig. 4C). The anti-paraflagellar rod (PFR2) monoclonal L8C4 antibody was used as a loading control for western blotting and illustrates that equal numbers of cells were loaded in the western blot experiment (Fig. 4C).

The number and organisation of basal bodies in *Tb*NRKC-depleted cells, was checked by double labelling with an antibody specific to an axonemal protein (M25, our own unpublished monoclonal) and YL1/2. Seventy-two hours after induction, we observed that 1.0% of the RNAi population had mother and daughter flagella that remained close to each other, forming flagella pairs. Individual *Tb*NRKC-depleted cells would often have two or three of these mature pairs (Fig. 5A). Additionally, we observed a small population of cells with an isolated, non-flagellated basal body or clusters of basal bodies, all associated with an enlarged kinetoplast (Fig. 5B). These large kinetoplasts frequently maintained abnormal numbers of basal bodies associated with them and surprisingly, when probed with Mab25, these basal bodies had not formed flagella. Of the induced population, 0.4% had one or more clusters of basal bodies, (Fig. 5D) and 4.6% had more than four basal bodies (three, four or five mature basal bodies associated with three, four or five non-flagellated basal bodies). The dominant, unambiguous phenotype observed in the RNAi-induced culture was linked to basal body division. In RNAi-induced culture 46.2% of cells had two basal bodies (one mature and one immature) compared with 77.04% found in wild-type culture. Furthermore, 47.8% of induced cells had four basal bodies (two mature and two immature) compared with 22.2% in wild-type cells (Fig. 5C,D). These data illustrate a 'four-basal-body' accumulation effect stimulated by the loss of *Tb*NRKC protein. FACS analysis of the RNAi *Tb*NRKC-knockdown cells indicated that after 72 hours of RNAi induction, the percentage of cells in G1 decreased from

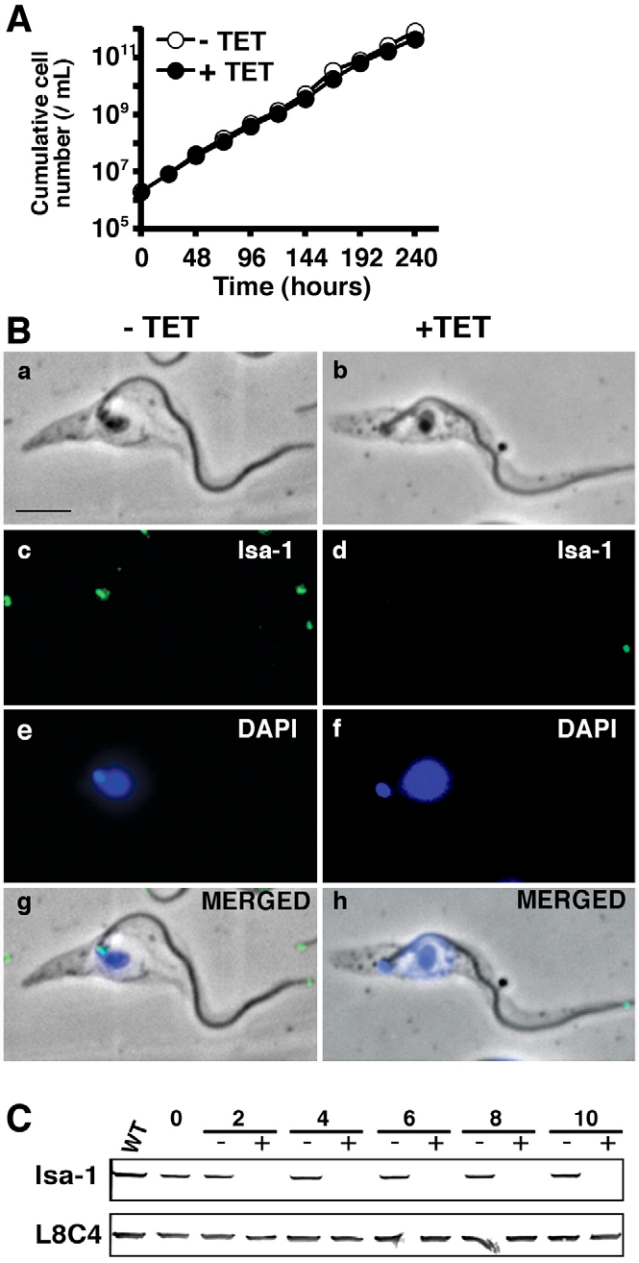

Fig. 4. (A) Growth curve of *Tb*NRKC RNAi-induced cells. Knockdown of *Tb*NRKC is not lethal and cell growth is similar to non-induced cultures up to 10 days after induction. (B) Isa-1 immunofluorescence signal is present in non-induced cells (–TET) on the basal body (c). 48 hours after induction, Isa-1 signal is lost in RNAi-induced cells (+TET) (d). a,b, phase-contrast images. Bar, 5 μm. (C) *Tb*NRKC levels analysed by western blot after RNAi induction (in days). 2 days of induction (+) is sufficient to deplete cells of *Tb*NRKC protein. No reappearance of *Tb*NRKC protein is detected up to 10 days of induction. The transformed cell line at time zero (0) or non-induced cells (–) express similar amounts of *Tb*NRKC protein as wild-type cells (WT). Membranes were probed with Isa-1 (upper panel) or with L8C4 as a loading control (lower panel). 2.5×10^{6} cells/well were loaded.

61.17% (WT cells) to 51.83%. The percentage of cells in S phase remained stable (11.23% WT, 12.83% RNAi). The percentage of cells in G2-M phase increased (from 24.93%

WT to 28.78% RNAi). The percentage of cells with abnormally high DNA content also increased (from 3.02% WT to 6.87% RNAi) (Fig. 5E). These results show very little change in DNA content between wild-type and RNAi-knockdown cells indicating that knockdown cells did not undergo cell-cycle arrest and show a minor enrichment in G2 cells. These results suggest a slight delay in G2, with the production of a minor population of cells with aberrant ploidy.

Overexpression of *Tb*NRKC is lethal and prevents basal body separation and cytokinesis

Full-length, non-tagged and various tagged versions of the protein were expressed in procyclic cells (NRKC, TY1-NRKC and NRKC-GFP) under the control of the tetracycline repressor. For the three constructs described above we observed similar results and we have therefore only shown the results of TY1-NRKC overexpression. Confirmation of protein expression was done using western blotting with Isa-1 or the anti-TY1 monoclonal antibody BB2 (Fig. 6A, upper panel). Comparison of overexpressing and non-induced cell growth curves illustrated that induced cells stop dividing after 48 hours (Fig. 6A, lower panel). These cells showed very dramatic and distinct phenotypes. Cells were multinucleated and often had a large single kinetoplast (Fig. 6B,C; Fig. 7B). These large

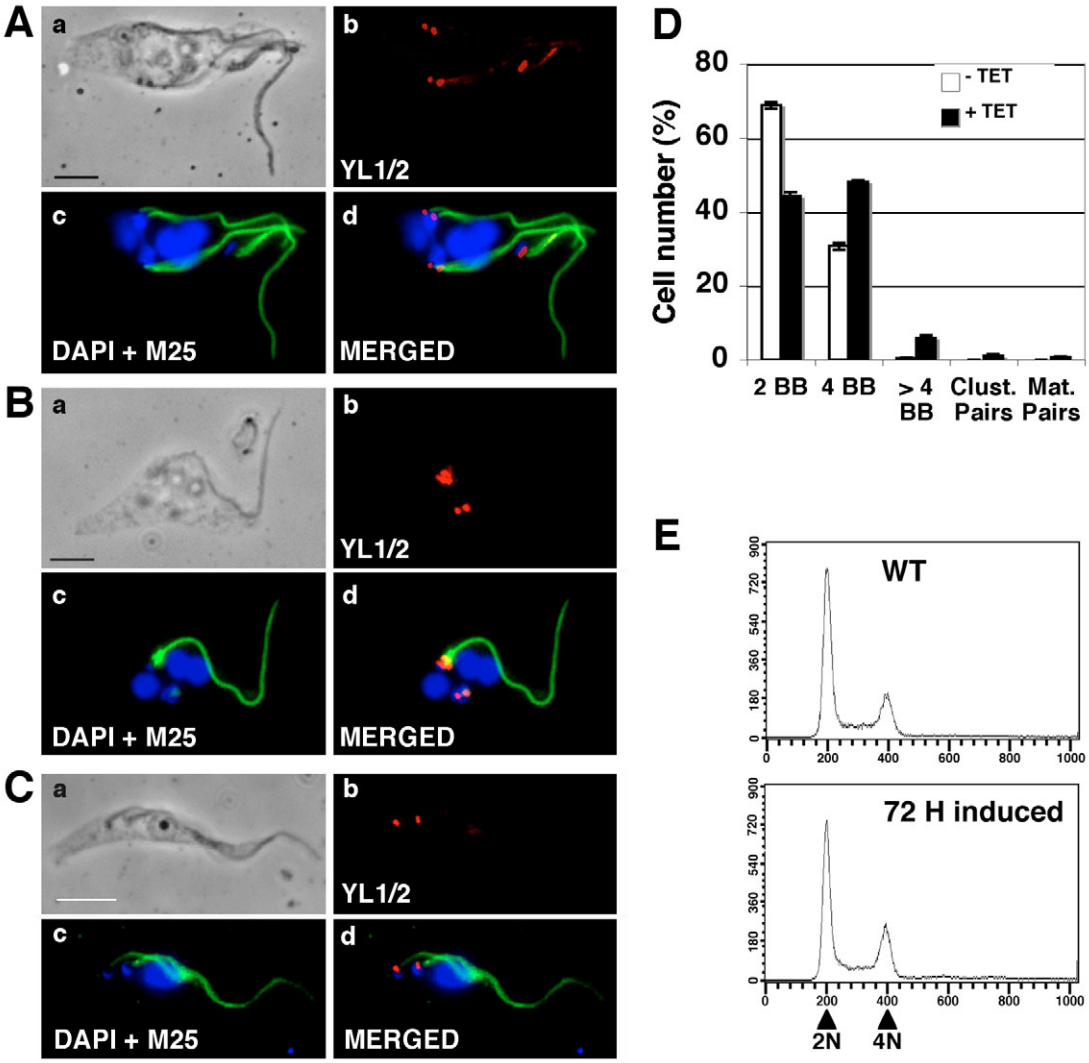

Fig. 5. Phenotypes induced by RNAi in procyclic cells. (A) A small population of cells (~1%) displayed flagella pairs. Cytoskeletons of cells induced for 48 hours probed with YL1/2 (b) and M25 plus DAPI (c). (B) A small population of cells displayed clusters of non-flagellated basal bodies. Cells were probed as in A. (C) A RNAi-induced four-basal-body cell, probed with YL1/2 (b) and M25 plus DAPI (c), illustrating a normal phenotype. Knockdown of *Tb*NRKC does not block basal body separation or cytokinesis. Bars, 5 μm. (D) Basal body counts of wild-type (WT) and *TbNRKC* RNAi-induced cells (+TET). After 72 hours of induction, 46.2% of the population had two basal bodies (2BB) compared with 77.04% of wild-type cells. 47.8% of induced cells had four basal bodies (4BB) (two mature and two immature) compared with 22.2% in wild-type cells. 4.6% displayed more than four basal bodies (>4BB), 0.4% displayed clustered basal bodies (Clust. BB) and 1% displayed mature flagella pairs (MAT. PAIRS). Values are mean ± s.e.m. of three experiments. (E) FACS analysis of RNAi knockdown cells. After 72 hours (72 H) of RNAi induction, the percentage of cells in G1 decreased from 61.17% (WT cells) to 51.83%. The percentage of cells in S-phase remained stable (11.23% WT, 12.83% RNAi). The percentage of cells in G2-M phase increased (from 24.93% WT to 28.78% RNAi). The percentage of cells with abnormally high DNA content also increased (from 3.02% WT to 6.87% RNAi).

kinetoplasts maintained abnormal numbers of basal bodies. When probed with Mab25 these basal bodies had not formed flagella after at least two rounds of the cell cycle (Fig. 6B). Furthermore, they were randomly localised on or near the kinetoplast. At 96 hours of induction, 80.8% of cells possessed at least one large kinetoplast and more than two nuclei (Fig. 6C). We then investigated the number and location of basal bodies in overexpressing cells by immunofluorescence using YL1/2. In wild-type cells, 77.04% had two basal bodies and 22.2% had four basal bodies. At time 0, 73.4% of induced cells had two basal bodies and 26.3% had four basal bodies. However, 96 hours after induction, 11.2% of induced cells had two basal bodies, 13.6% had four basal bodies, 17.7% of cells had more than four basal bodies of which 4.6% had more than eight basal bodies. Strikingly, 57.4% of cells had clusters of numerous non-flagellated basal bodies (Fig. 6B,D). The ability of basal bodies to form flagella in these cells appears to be blocked.

Ultra-thin sections of induced overexpressing TY1-NRKC cells (72 hours) illustrated that basal bodies were clustered in groups and were indeed associated with an enlarged kinetoplast (Fig. 7B). This is in contrast to wild-type cells where post-mitotic mature basal bodies are approximately 6 μm apart (Robinson et al., 1995). Additionally, the basal bodies of wild-type cells are connected to the replicating kinetoplast by the tripartite attachment complex (TAC) (Ogbadoyi et al., 2003). The cytoplasmic portion of the zone within the TAC consists of linkage fibres known as the exclusion zone filaments. The presence of this exclusion zone between basal body and kinetoplast is a good indication that these two organelles are physically linked (Fig. 7A) (Ogbadoyi et al., 2003). Cells overexpressing TY1-NRKC had large disorganised exclusion

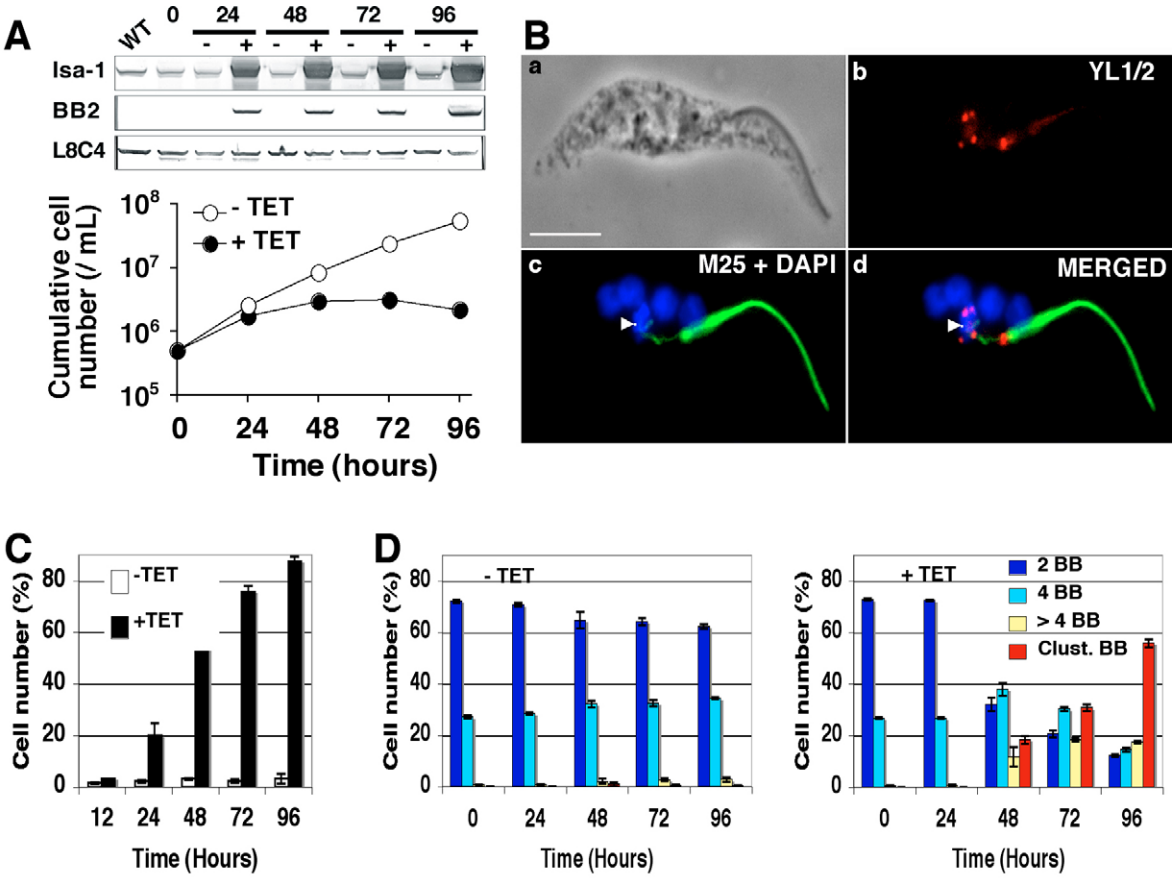

Fig. 6. Overexpression of TY1-NRKC blocks cytokinesis. (A, top panel) Western blot of overexpressed TY1-NRKC protein (time in hours). The membrane was probed with Isa-1 and indicates the increased concentration of TY1-NRKC of protein observed in induced (+) cells. The blot was also probed with the anti-TY1 tag antibody BB2. Wild-type cells (WT), induced time 0 or non-induced (–) cells did not express the tagged protein. TY1-NRKC is observed after 24 hours of induction as illustrated in (+) lanes. The blot was probed with anti-PFRA monoclonal L8C4 as a loading control. Blots were loaded with 5×10^6 cells/lane. (A, bottom panel) Comparative growth curves of non-induced (– TET) and induced cells (+ TET) indicate that cells overexpressing TY1-NRKC have a reduced growth rate compared with non-induced cells. (B) Cytoskeletons of TY1-NRKC cells induced for 48 hours were probed by immunofluorescence with YL1/2 (b) and M25 (c). This multinucleated cell possesses one flagellum but four basal bodies (b and d), indicating that the cell passed through the cell cycle the absence of cytokinesis. The arrowheads in c and d indicate a large kinetoplast close to the basal bodies. Bar, 5 μm. (C) Counts of cells possessing at least one large kinetoplast and more than two nuclei in non-induced (– TET) and induced cells (+ TET) from 0 to 96 hours. After 96 hours of induction, 80.8% of cells possessed at least one large kinetoplast and more than two nuclei. (D) Populations of non-induced (– TET) and induced (+ TET) cultures were assessed to identify the percentage of cells possessing two basal bodies (2 BB), four basal bodies (4 BB), more than four basal bodies (>4 BB) and clusters of non-flagellated basal bodies (Clust. BB). Assessment was done from 0 to 96 hours of TY1-NRKC induction. All values are mean ± s.e.m. of three experiments.

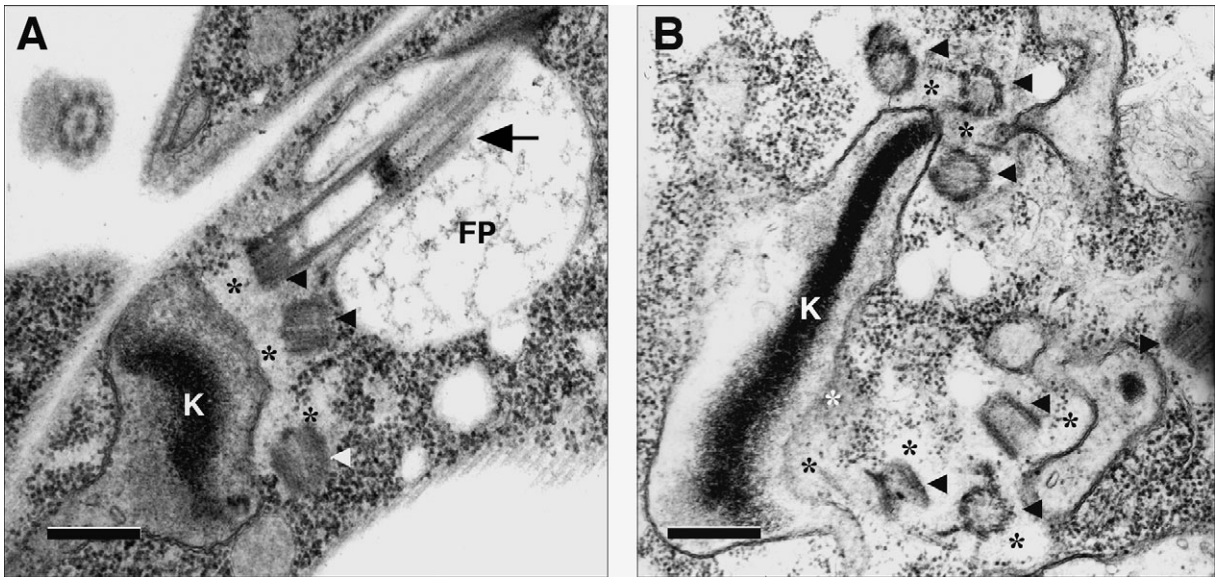

Fig. 7. (A) Longitudinal section of a TY1-NRKC non-induced cell illustrating the mature flagellum (arrow), its mature basal body (upper black arrowhead) and its immature pro-basal body (lower black arrowhead). This cell is in the early stages of kinetoplast replication and possesses a second immature pro-basal body (lower white arrowhead), which is linked to a second flagellum (not within the plane of this section). (B) Longitudinal section of a TY1-NRKC-induced cell (72 hours). The section traverses a cluster of seven basal bodies (arrowheads). At least three non-flagellated basal bodies can be observed. The kinetoplast is larger than wild-type cells (at least 3 μm in diameter). K, kinetoplast; FP, flagellar pocket. Asterisks indicate ribosome-free regions of the TAC. Bars, 500 nm.

zones present between the basal bodies and the kinetoplast demonstrating that these organelles were probably physically linked to each other (Fig. 7B). The kinetoplasts of overexpressing cells were much larger than wild-type cells, indicating that they had passed through at least one round of DNA S phase without adequate division (Fig. 7B).

Overexpression of kinase-dead *Tb*NRKC

In order to investigate whether kinase activity was required to block cytokinesis and/or basal-body-mediated flagella development we overexpressed an inactive form of *Tb*NRKC (mNRKC-6His). In this kinase-dead protein the amino acid Lys33 of the kinase domain was mutated to methionine. Overexpression of the protein was confirmed by western blot (Fig. 8A). Growth curves of cells transformed to express this protein were carried out on non-induced and induced cultures. Cells overexpressing kinase-dead protein showed only a slightly reduced growth rate 96 hours after induction (Fig. 8A). However, the ratio of cells with two or four basal bodies in induced cells changed dramatically 96 hours after induction with 48.57% of induced cells having two basal bodies (one mature and one immature) compared with 63.28% in the non-induced culture (Fig. 8B) and 77.04% in wild-type cultures (Fig. 5D). Furthermore, 47.04% of induced cells had four basal bodies (two mature and two immature) rather than the 35.78% in the non-induced cells or the 22.2% in wild-type cells (Fig. 8B,C). A cell overexpressing kinase-dead protein with four basal bodies is shown in Fig. 8C.

Discussion

We have identified a new member of the NEK family, *Tb*NRKC, which is a basal body protein. The *Tb*NRKC protein contains all of the conserved sub-domains present in the protein kinase family. In similarity searches using the kinase domain of *Tb*NRKC we found that it had strong identity with human NEK1 (50%) and shares 42% identity with human NEK2. It has structural similarities to NEK2 and is a true kinase. *Tb*NRKC is located on mature and immature basal bodies and is the first *T. brucei* NRK to be found associated with the cytoskeleton. We have also shown in this work that overexpression of active, but not inactive, *Tb*NRKC blocks flagella formation and thus cytokinesis. The absence of *Tb*NRKC in the cell stimulates the accumulation of a four-basal-body phenotype. NEK2 of mammalian cells is involved in the dislocation of an important centriolar protein C-Nap1. Upon phosphorylation, C-Nap1 is displaced from the centriole and splitting occurs (Faragher and Fry, 2003; Fry et al., 1998b). Rootletin, another centriole protein, forms centriole-associated filaments, interacts with C-Nap1 and functions in centrosome cohesion. It is also phosphorylated by NEK2 (Bahe et al., 2005). No rootletin or C-Nap1 homologues have been identified in the *T. brucei* genome database but these cells must clearly require functional equivalents.

Basal body separation is a physical marker or checkpoint for trypanosomes (Ploubidou et al., 1999). A NEK-like protein, with tubulin glutamylation activity (*Cf*NEK) has been identified in *Crithidia fasciculata*. Interestingly, it is located on the proximal end of both mature and immature basal bodies and the FAZ (Westermann and Weber, 2002). GFP-tagged *Tb*NRKC has a transition zone signal, which could suggest that in these cells the transition zone signal is not artifactual. However, we cannot rule out the hypothesis that excess GFP-tagged protein may enter the lumen of the mature basal body. The role of *Cf*NEK in the cell cycle is yet to be determined. A NIMA-related kinase Fa2p has been identified on basal bodies in *Chlamydomonas reinhardtii* (Mahjoub et al., 2002; Mahjoub

et al., 2004). Fa2p has only 9% overall amino acid identity with *Tb*NRKC but 37% amino acid identity over the kinase domain. Fa2p is located at the proximal ends of basal bodies, distal to the transition zone, but is also on the proximal ends of dubicaine-induced detached flagella. Mutations in the *FA2* gene produced a retardation of the cell cycle resulting in large cells, suggesting that the Fa2p protein can influence cytokinesis.

RNAi knockdown of *Tb*NRKC in procyclics produced 47.8% of cells that have four basal bodies rather compared with 22.2% in wild-type cells, suggesting that knockdown of *Tb*NRKC protein can modify the progression of cells through the cell cycle and stimulate an accumulation of cells at this stage. This phenomenon was also observed in the cells overexpressing kinase-dead *Tb*NRKC suggesting a dominant-negative effect of the inactive protein. However, in both RNAi knockdown and kinase-dead experiments, the cell cycle was not completely blocked. At least 20 NEK proteins have been identified in the *T. brucei* genome, a surprisingly large number, considering the 15 or so present in humans (Parsons et al., 2005). These NEKs have not been characterised in detail. However, one or more of these proteins could conceivably rescue *Tb*NRKC RNAi-knockdown cells.

Overexpression of kinase-dead NEK2 or its C-terminus in mammalian cells or *Dictyostelium*, resulted in the splitting of centrosomes or the formation of supernumerary MTOCs, indicating that the C-terminus, rather than the kinase domain is responsible for the formation of the supernumerary MTOCs (Faragher and Fry, 2003; Fry et al., 1998a; Graf, 2002). Overexpression of active *Tb*NRKC initiates the formation of supernumerary basal bodies. Their formation resulted from continued basal body formation in the absence of correct cytokinesis. However, overexpression of kinase-dead protein produced RNAi-knockdown-like phenotypes with an accumulation of cells with four basal bodies. This data indicates that: (1) the C-terminus of *Tb*NRKC does not have a role in the formation of supernumerary basal bodies when over-expressed in vivo; (2) absence of kinase activity results in a delay of basal body separation. We propose that cells overexpressing active *Tb*NRKC do not separate their pro-basal or supernumerary basal bodies because they do not form flagella. We have previously shown that in the absence of flagella, basal body and kinetoplast segregation is blocked (Kohl et al., 2003). It is not clear why flagella do not form on the pro-basal or supernumerary basal bodies in cells overexpressing active *Tb*NRKC. It is possible that in these cells overexpression of active *Tb*NRKC can prematurely stimulate the disassociation of the links between pro-basal and mature basal bodies. If this occurs, the cell could continue through one or more cell cycles without dividing and produce numerous pro-basal (supernumerary) basal bodies. These basal bodies are unable to form flagella as they may require additional proteins or modifications that would normally function at a later time point in the cell cycle, or after the pro-basal bodies reach a defined maturity status. There are no biochemical or immunological markers available that can clearly discriminate between a mature basal body a pro-basal or supernumerary basal body. Therefore, we cannot define biochemically, the maturity status of basal bodies. Nevertheless, because flagella are required for basal body separation these supernumerary basal bodies are unlikely to separate correctly.

The accumulation of four basal bodies in RNA knockdown or kinase-dead experiments, implies that the activity of *Tb*NRKC is most important for cells at the four-basal-body stage. We hypothesise that, in wild-type cells, *Tb*NRKC is an activator of basal body separation and is involved in the removal, disassociation or disassembly of the linkages present

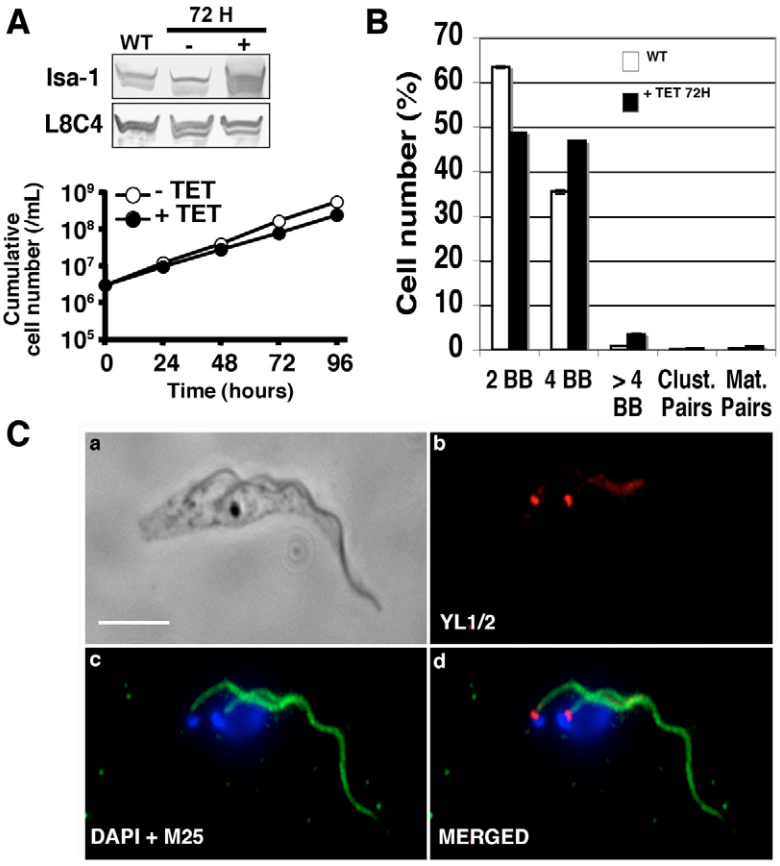

Fig. 8. Overexpression of kinase-dead *Tb*NRKC in vivo. (A, top panel) Western blot of wild-type (WT), non-induced (–) and induced cells (+) for 72 hours. The membrane was probed with Isa-1 and indicates the overexpression of mNRKC in induced cells. (A, bottom panel) Growth curve of non induced (–) and induced cells (+). (B) Basal body counts of non-induced (– TET) and induced cells (+TET). After 72 hours of induction, 48.57% of induced cells had two basal bodies (2BB) compared with 63.28% of non-induced cells. 47.04% of induced cells had four basal bodies (4BB) (two mature and two immature) compared with 35.78% of non-induced cells. In induced cells 3.63% (0% for non induced) displayed more than four basal bodies (>4BB), 0.19% (0% for non induced) displayed clustered basal bodies (Clust. BB) and 0.57% displayed mature flagella pairs (MAT. PAIRS). (C) A cell overexpressing kinase-dead *Tb*NRKC in vivo probed with YL1/2 (b) and M25 plus DAPI (c), illustrating the four-basal-body phenotype. Bar, 5 μm.

between the mother basal body and the newly matured basal body. Precisely coordinated kinase activity is required for the correct disassembly process of the link between these basal bodies. Several models can be made as to the timing of the initiation of *Tb*NRKC activity. Activity may be initiated immediately after the formation of the four-basal-body cell cycle stage or later on in the cell cycle, when the cell has two flagella (a mature old and a short new flagellum). Alternatively, activity may be constitutive, but access to the protein substrate(s) may be blocked until a specific point in the cell cycle is reached. Our observations of cells overexpressing active kinase illustrate that supernumerary flagellar-less basal bodies are formed and cytokinesis is blocked. This suggests that in these cells disassembly of the pro-basal-body to mature-basal-body link at very early stages in the cell cycle, can influence flagella formation and cytokinesis. We thus support the hypothesis that activity of NRKC in wild-type cells is most important early in the cell cycle, immediately after the four-basal-body stage. Since trypanosomes cannot be synchronised, a more precise characterisation of the timing of activity is currently not feasible.

In the early stages of the wild-type cell cycle two pro-basal bodies are formed immediately after construction of the transition zone of the maturing basal body. Thus each individual pro-basal body is physically linked to a mature basal body. However, these recently formed links are not stimulated to disassociate by wild-type levels of *Tb*NRKC. In the subsequent cell cycle however, this link is recognised and is activated for disassociation. This indicates the existence of precise physical targeting of *Tb*NRKC activity to the links between mature basal bodies. Mature basal body separation is then achieved through microtubule-mediated processes. To date no data has been published indicating that *T. brucei* is able to divide in the absence of basal bodies or flagella. The roles played by flagella and basal bodies in controlling trypanosome cytokinesis are clearly important and it appears probable that the basal body checkpoint and/or marker is difficult or impossible to override and that these cells are under the control of a flagellum-basal body linked cytokinesis restraint.

NEK-NEK interactions both physically and within the context of the cell cycle have been reported (Belham et al., 2003). The *Tb*NRKC is probably under precise and selective temporal control during the cell cycle and may interact with other NEKs. Since many eukaryotes have centrioles rather than basal bodies (Marshall and Rosenbaum, 2000), it is interesting to note that the localisation and function of some NEKs has been conserved to these unique organelles.

Materials and Methods

Identification of *Tb*NRKC and construction of plasmids

The *TbNRKC* gene was identified from the (TIGR) trypanosome genome project, (www.genedb.org). We used the human *Hs*Nek2 protein (GenBank accession number P51955) or *A. Nidulans* NIMA protein (P11837) as queries. *TbNRKC* was amplified by polymerase chain reaction (PCR) from *T. brucei* 927 genomic DNA with the primers N1-*Xba*I (5′-CCCTAGTCTAGACCGCAGCATTTGACGATT-AAATGC-3′) and N1-*Xho*I (5′-CCCCCGCTCGAGATGGAGAATTACACCCAA-CTTCGTG-3′). The PCR product was sequenced and displayed two different alleles. One allele was identical to the sequence from the database. The second allele had three silent mutations (C28T, G762A, G2214A) and a point mutation W(TGG)428R(CGA) when compared with the TIGR sequence. The cloned *TbNRKC* gene carries the W428 residue and the silent mutations. For expression of NRKC-GFP fusion protein in procyclics, the PCR product above was ligated between the *Xba*I-*Xho*I sites of pLew79-GFP1 plasmid (Coustou et al., 2005). The construct named p79NrkC-GFP was used as a DNA template for the following: an N-terminal, TY1-tagged *Tb*NRKC (TY1-NRKC) (Bastin et al., 1996) using the primers *Hin*dIII-TY-N1 (5′-AAACCCAAGCTTATG**GAGGTCCATACTAACCA-GGACCCACTTGAC**ATGGAGAATTACACCCAACTTCGTGTG-3′) containing the TY1 sequence (bold) and *Bam*HI-N1 (5′-CCCCGCGGATCCTTACCGCAG-CATTTGACG-3′) and cloned into the procyclic expression vector pLew79 (Wirtz et al., 1999) between the *Hin*dIII and *Bam*HI sites to generate p79TY-NrkC. An N-terminal truncated version of *Tb*NRKC (6HIS-tNRKC) was used to make antiserum. A fragment corresponding to nucleotides 810-2292 of *TbNRKC* (amino acids 270-764) was amplified by PCR using the primers His-N1-*Xho*I (5′-GGTGGT-CTCGAGGATGCCCACAATAATAAAGGG-3′) and *Bam*HI-N1 (5′-CCCCGC-GGATCCTTACCGCAGCATTTGACG-3′) and cloned between the *Xho*I and *Bam*HI sites of the pET16b vector (Novagen) to generate p16tNrkC. For the kinase assay, the full-length *Tb*NRKC protein was expressed with a histidine tag on the C-terminus (NRKC-6His). The *TbNRKC* sequence was amplified by PCR using the primers N1-*Hin*dIII (5′-GGGCCCAAGCTTATGGAGAATTACACCCAACTTC-GTG-3′) and *Xho*I-pET28-N1H (5′-CCCCCGCTCGAGCCGCAGCATTTGAC-GATTAAATGC-3′) and cloned in the pET28a(+) expression vector (Novagen) between the *Hin*dIII and *Xho*I sites to generate the p28NrkC plasmid. From p28NrkC, we generated the kinase-dead *TbNRKC* (mNRKC-6His) by mutating Lys33 to Met using the QuikChange site-directed mutagenesis kit (Stratagene) and the mutagenic 35-mer oligonucleotide K33MN1S (5′-CGTGAAGTTTGTAGC-TATGGAGGTGAGATTAGCCG-3′, mutated bases are underlined) with the corresponding complementary antisense primer K33MN1AS (5′-CGGCTAAT-CTCACCTCCATAGCTACAAACTTCACG-3′) according to the manufacturer's instructions. The plasmid was named p28mNrkC and the mutation was confirmed by DNA sequencing. To express the kinase-dead *Tb*NRKC in vivo, the mutated gene was amplified from the p28mNrkC plasmid with primers N1-*Hin*dIII and N1-*BamH*I and cloned between the *Hin*dIII-*Bam*HI sites of pLew100 (Wirtz et al., 1999) to generate p100mNrkC. The RNAi stem-loop construct was generated as follows. A first fragment of 640 bp was amplified with the primers N1-*Hd3-RNAiult* (5′-CAGAAGAAGCTTGGCGACGAGCACTGGC-3′) and N1-Xba1-TBult (5′-CAG-TTGTCTAGAGATTGGGATGTATTTATGG-3′) and ligated between the *Hin*dIII and *Xba*I sites of pLew79 (p79NrkCs). The second 693 bp fragment was generated with the primers N1-*Xba*1 (5′-ccctagtctagaCCGCAGCATTTGACGATTAAATGC-3′) and N1-*BH*1-RNAiult (5′-CAGAAGGGATCCGGCGACGAGCACTGGC-3′). This fragment was ligated in p79NrkCs between the *Xba*I and *Bam*HI restriction sites to produce the plasmid p79NrkCRNAi. PCR products or cloned fragments were checked by sequencing. The nucleotide sequence of *TbNRKC* reported in this paper has been deposited at GenBank accession number DQ054526.

Cell lines and transfections

The *T. brucei* EATRO 1125 and EATRO1125-T7T procyclic strains used are described (Bringaud et al., 2000; Delauw et al., 1985). Bloodstream forms were Antat1.1E, a kind gift from George Cross (Rockefeller University, New York). Procyclic *T. brucei* cells were grown at 27°C in SDM-79 (Brun and Schonenberger, 1979) containing 10% (v/v) heat-inactivated foetal bovine serum and 3.5 mg/ml hemin (Complete Medium). Cells were used between 2×10^6 cells/ml and 1×10^7 cells/ml. EATRO1125 T7T procyclic strain was used for transfections. These were grown in Complete Medium supplemented with 10 μg/ml of G418 and 25 μg/ml hygromycin and were transformed by electroporation with 10 μg *Not*I-linearised vectors as described (Bringaud et al., 1998). After 24 hours, transfected cells were diluted in conditioned Complete Medium containing 20% FCS and the antibiotics G-418 sulphate (10 μg/ml), hygromycin (25 μg/ml) and phleomycin (5 μg/ml) and dispensed into a 24-well plate. After 10 to 20 days, transformants were screened, after tetracycline induction (10 μg/ml), by immunofluorescence and cloned by serial dilution.

Expression and purification of recombinant proteins

To produce the recombinant proteins 6His-tNRKC, NRKC-6His or mNRKC-6His, a 500 ml culture (in LB medium supplemented with 50 μg/ml kanamycin or 100 μg/ml ampicillin) of *E.coli* BL21(DE3) transformed with the plasmids pET16-His-NEK1, pET28-NEK1-His or pET28-NEK1-HisK33M was induced for 3 hours at 37°C with 1 mM isopropyl-β-thiogalactopyranoside. Cells were harvested (1000 ***g***, 15 minutes) and the pellet was resuspended in Buffer A (50 mM Tris-HCl pH 7.5, 300 mM NaCl) with 1 mM PMSF and complete Mini EDTA-free protein inhibitor cocktail (Roche). Cells were lysed by sonication and the lysate was centrifugated at 10,000 ***g*** for 1 hour at 4°C. Recombinant proteins were purified by nickel chelate affinity chromatography using Ni-NTA agarose (Qiagen). After washing in Buffer A, Buffer A + 10 mM imidazole then Buffer A + 50 mM imidazole, the proteins were eluted with 250 mM imidazole in Buffer A as 1.4 ml fractions into 0.6 ml of 100% glycerol (30% final concentration) then stored at –80°C.

Antibody production

The 6His-tNRKC purified recombinant protein was electroeluted from a 12% SDS-PAGE gel or was dialysed against 50 mM Tris-HCl pH 7.5. The polyclonal Isa-1 was made after two Balb/C mice were immunised with a mixture of 50 μg of electroeluted protein and 50 μg of dialysed protein.

Western blotting

Whole cells were prepared as described (Laemmli, 1970). *T. brucei* procyclic or bloodstream cells (2.5-5×10^6 cells/well) were separated by SDS-PAGE (10%) and transferred onto PVDF membrane. Membranes were blocked in Tris-buffered saline (TBS), 0.2% Tween-20, 5% skimmed milk powder for 1 hour, incubated overnight at 4°C with the primary antibodies Isa-1, L8C4 (Kohl et al., 1999) or BB2 (Bastin et al., 1996) diluted in blocking solution at 1:25,000, 1:1000 and 1:25, respectively. After washing in 1 M NaCl and in TBS, 0.2% Tween-20, the membranes were incubated with sheep anti-mouse IgG alkaline-phosphatase-conjugated secondary antibody (Jackson) (1:40,000 in TBS, 0.2% Tween-20) or with goat anti-mouse IgG and IgM HRP (horseradish peroxidase)-conjugated secondary antibody (Jackson) at 1:20,000 in TBS, 0.2% Tween-20 for 1 hour at room temperature. After washes in TBS, 0.2% Tween-20 then TBS, membranes were incubate in alkaline phosphatase buffer for 10 minutes and revealed with BCIP/NBT-blue liquid substrate system for membranes (Sigma) or washed in TBS and revealed with 0.05% diaminobenzidine, 0.015% H_2O_2.

Immunofluorescence and direct GFP fluorescence

Cells were washed in PBS pH 7.4 and spread on poly-L-lysine-coated slides. Cytoskeletons were extracted in PBS, pH 7.4, 0.25% NP40 or 0.25% NP40 in 100 mM PIPES, 1 mM $MgCl_2$, pH 6.9, for 5 minutes, fixed in 2% paraformaldehyde in PBS for 5 minutes neutralised with 100 mM glycine for 10 minutes. Primary antibodies used were: anti-PFR2 monoclonal L8C4 (Neat), Isa-1 (1:600 in PBS, 2% BSA, 0.1% Tween-20), monoclonals Mab25 made in our lab (1:40 in PBS) against a *T. brucei* axoneme protein (our unpublished data) or Mab22 (neat), made against a *T. brucei* basal body protein (our unpublished data), or rat IgG2a monoclonal YL1/2 anti-tyrosinated tubulin (Abcam ab6160, 1:500 dilution in PBS), Secondary antibodies; FITC-conjugated goat anti-mouse IgG (Sigma) or Oregon Green®488 goat anti-mouse IgG (H+L) (Molecular Probes) or Alexa Fluor®594 chicken anti-rat IgG (H+L) (Molecular Probes) at 1:100 in PBS. For immunofluorescence of *Tb*NRKC-GFP overexpressing cells, cytoskeleton were extracted in 0.1% or 0.2% NP40 in 100 mM PIPES, 1 mM $MgCl_2$, pH 6.9, 5 minutes and fixed as above. Double labelling experiments; primary antibodies were rabbit IgG anti-GFP (Molecular Probes, 1:200) and YL1/2 as above, followed by FITC-conjugated goat anti-rabbit IgG secondary antibody (Sigma, 1:100 dilution in PBS) and Alexa Fluor®594 chicken anti-rat IgG secondary antibody. Direct fluorescence of *Tb*NRKC-GFP protein; procyclic cells were washed and spread as above, probed with DAPI and mounted in Slowfade (Molecular Probes). All cell counts were done in triplicate (three cultures) with a minimum of 500 cells.

Isa-1 polyclonal antibody saturation assays

Isa-1 mouse polyclonal antibody (20 μl; 1:150 in PBS) was incubated with 20 μl recombinant NRKC-6HIS protein (130 ng/μl final concentration) at 4°C overnight. The recombinant protein (bound or not bound to the antibody) was centrifuged for 15 minutes at 16,000 ***g***, 4°C, or eliminated by adding 5 μl of Ni-NTA agarose slurry and incubating for 1 hour at 4°C before centrifugation as before. The supernatant was used neat for the immunofluorescence and diluted for the western blot or as described previously.

Kinase assays

Kinase reactions (30 μl) were performed in kinase buffer (20 mM Tris-HCl, pH 7.5, 20 mM $MgCl_2$, 2 mM $MnCl_2$) containing 0.7 μg NRKC-6His or mNRKC-6His, 10 μM ATP (Invitrogen), 5 μCi [^{32}P]ATP (3000 Ci/mmol) (Amersham Biosciences), 5 μg dephosphorylated α/β casein substrate (Sigma) or BSA as negative control. The reactions were incubated at 30°C for 30 minutes and stopped by the addition of 10 μl of 4× Laemmli sample buffer and heated for 3 minutes at 100°C. Protein samples (15 μl) were resolved by 10% SDS-PAGE. Gels were dried and exposed to X-ray film (Kodak BioMax Light Film).

Fluorescence-activated cell Sorting (FACS) analysis

Cell samples for FACS analysis were prepared as described (Tu and Wang, 2004). The DNA content of propidium-iodide-stained cells was analysed with a FACSCalibur analytical flow cytometer. The percentage of cells in each phase of the cell cycle (G1, S and G2-M) was determined by CellQuest software.

Electron microscopy

EATRO1125T7T cells and TY1-NRKC-expressing cells were grown in Complete medium supplemented with the antibiotics hygromycin, G418, phleomycin and tetracycline for the induced TY1-NRKC overexpressing cell line. Non-induced and wild-type cells were mock treated. Cells were harvested by and fixed in 25 ml of 4% paraformaldehyde, 4% glutaraldehyde, 0.2% tannic acid in 0.1 M cacodylate buffer pH 7.0 at room temperature for 2 hours, then post-fixed in osmium tetroxide, block stained in 2% uranyl acetate, dehydrated and embedded in Spurr's resin (Spurr, 1969). Sections were visualised on a Philips CM10 electron microscope.

Immuno-electron microscopy

EDTA was added at a final concentration of 10 mM to a 10 ml mid-log phase culture of *T. brucei* (EATRO 1125). Cells were harvested and washed in PBS, resuspended in 500 μl PBS and placed on Parafilm. Charged formvar carbon-coated grids (EMS G200-Ni) were floated onto the droplet for 30 minutes. Grids were transferred to 500 μl PBS, 10 mM EDTA, 0.5% NP40 for 15 minutes then washed three times for 15 minutes with 500 μl PBS, 10 mM EDTA. Flagella were fixed (4% paraformaldehyde, 0.01% glutaraldehyde in PBS, 30 minutes), washed in 100 mM glycine three times for 5 minutes and blocked in 2% BSA in PBS twice for 10 minutes. Grids were incubated (45 minutes) in Isa 1, 1:300 dilution in PBS, 2% BSA, 0.1% Tween 20, washed five times for 10 minutes in incubation buffer and incubated for 45 minutes on 35 μl of 10 nm gold conjugate (BBL, EMGMHL10), 1:30 in incubation buffer. They were then washed four times for 10 minutes in incubation buffer, four times for 10 minutes in PBS, fixed for 1 minute in 1% glutaraldehyde and negatively stained (NanoVan, Nanoprobes; 5 μl/grid).

We thank The Baltz laboratory. Keith Gull (University of Oxford) for L8C4 and BB2 antibodies. Phillipe Bastin (Institut Pasteur), Jeremy Mottram and Tansy Hammarton (Wellcome Centre for Molecular Parasitology, Glasgow), for comments. Also, IFR 66 and Vincent Pitard for the use of the FACS machine. This work was funded by ATIP (CNRS), ACI, and Programme Protéomique et Génie des Protéines (CNRS) grants awarded to D.R. and a MRT fellowship awarded to L.P.

References

Bahe, S., Stierhof, Y. D., Wilkinson, C. J., Leiss, F. and Nigg, E. A. (2005). Rootletin forms centriole-associated filaments and functions in centrosome cohesion. *J. Cell Biol.* **171**, 27-33.

Bastin, P., Bagherzadeh, Z., Matthews, K. R. and Gull, K. (1996). A novel epitope tag system to study protein targeting and organelle biogenesis in Trypanosoma brucei. *Mol. Biochem. Parasitol.* **77**, 235-239.

Belham, C., Roig, J., Caldwell, J. A., Aoyama, Y., Kemp, B. E., Comb, M. and Avruch, J. (2003). A mitotic cascade of NIMA family kinases. Nercc1/Nek9 activates the Nek6 and Nek7 kinases. *J. Biol. Chem.* **278**, 34897-34909.

Bringaud, F., Baltz, D. and Baltz, T. (1998). Functional and molecular characterization of a glycosomal PPi-dependent enzyme in trypanosomatids: pyruvate, phosphate dikinase. *Proc. Natl. Acad. Sci. USA* **95**, 7963-7968.

Bringaud, F., Robinson, D. R., Barradeau, S., Biteau, N., Baltz, D. and Baltz, T. (2000). Characterization and disruption of a new *Trypanosoma brucei* repetitive flagellum protein, using double-stranded RNA inhibition. *Mol. Biochem. Parasitol.* **111**, 283-297.

Brun, R. and Schonenberger, M. (1979). Cultivation and in vitro cloning or procyclic culture forms of *Trypanosoma brucei* in a semi-defined medium. Short communication. *Acta Trop.* **36**, 289-292.

Chappuis, F., Loutan, L., Simarro, P., Lejon, V. and Buscher, P. (2005). Options for field diagnosis of human African trypanosomiasis. *Clin. Microbiol. Rev.* **18**, 133-146.

Coustou, V., Besteiro, S., Riviere, L., Biran, M., Biteau, N., Franconi, J. M., Boshart, M., Baltz, T. and Bringaud, F. (2005). A mitochondrial NADH-dependent fumarate reductase involved in the production of succinate excreted by procyclic *Trypanosoma brucei*. *J. Biol. Chem.* **280**, 16559-16570.

Delauw, M. F., Pays, E., Steinert, M., Aerts, D., Van Meirvenne, N. and Le Ray, D. (1985). Inactivation and reactivation of a variant-specific antigen gene in cyclically transmitted *Trypanosoma brucei*. *EMBO J.* **4**, 989-993.

Faragher, A. J. and Fry, A. M. (2003). Nek2A kinase stimulates centrosome disjunction and is required for formation of bipolar mitotic spindles. *Mol. Biol. Cell* **14**, 2876-2889.

Fry, A. M. (2002). The Nek2 protein kinase: a novel regulator of centrosome structure. *Oncogene* **21**, 6184-6194.

Fry, A. M., Mayor, T., Meraldi, P., Stierhof, Y. D., Tanaka, K. and Nigg, E. A. (1998a). C-Nap1, a novel centrosomal coiled-coil protein and candidate substrate of the cell cycle-regulated protein kinase Nek2. *J. Cell Biol.* **141**, 1563-1574.

Fry, A. M., Meraldi, P. and Nigg, E. A. (1998b). A centrosomal function for the human Nek2 protein kinase, a member of the NIMA family of cell cycle regulators. *EMBO J.* **17**, 470-481.

Fry, A. M., Descombes, P., Twomey, C., Bacchieri, R. and Nigg, E. A. (2000). The NIMA-related kinase X-Nek2B is required for efficient assembly of the zygotic centrosome in *Xenopus laevis*. *J. Cell Sci.* **113**, 1973-1984.

Gale, M., Jr and Parsons, M. (1993). A *Trypanosoma brucei* gene family encoding protein kinases with catalytic domains structurally related to Nek1 and NIMA. *Mol. Biochem. Parasitol.* **59**, 111-121.

Gale, M., Jr, Carter, V. and Parsons, M. (1994). Translational control mediates the developmental regulation of the *Trypanosoma brucei* Nrk protein kinase. *J. Biol. Chem.* **269**, 31659-31665.

Graf, R. (2002). DdNek2, the first non-vertebrate homologue of human Nek2, is involved in the formation of microtubule-organizing centers. *J. Cell Sci.* **115**, 1919-1929.

Hames, R. S., Wattam, S. L., Yamano, H., Bacchieri, R. and Fry, A. M. (2001). APC/C-mediated destruction of the centrosomal kinase Nek2A occurs in early mitosis and depends upon a cyclin A-type D-box. *EMBO J.* **20**, 7117-7127.

Hanks, S. K. and Quinn, A. M. (1991). Protein kinase catalytic domain sequence database: identification of conserved features of primary structure and classification of family members. *Methods Enzymol.* **200**, 38-62.

Hanks, S. K. and Hunter, T. (1995). Protein kinases 6. The eukaryotic protein kinase

superfamily: kinase (catalytic) domain structure and classification. *FASEB J.* **9**, 576-596.

Kilmartin, J. V., Wright, B. and Milstein, C. (1982). Rat monoclonal antitubulin antibodies derived by using a new nonsecreting rat cell line. *J. Cell Biol.* **93**, 576-582.

Kioy, D., Jannin, J. and Mattock, N. (2004). Human African trypanosomiasis. *Nat. Rev. Microbiol.* **2**, 186-187.

Kohl, L., Sherwin, T. and Gull, K. (1999). Assembly of the paraflagellar rod and the flagellum attachment zone complex during the *Trypanosoma brucei* cell cycle. *J. Eukaryot. Microbiol.* **46**, 105-109.

Kohl, L., Robinson, D. and Bastin, P. (2003). Novel roles for the flagellum in cell morphogenesis and cytokinesis of trypanosomes. *EMBO J.* **22**, 5336-5346.

Laemmli, U. K. (1970). Cleavage of structural proteins during the assembly of the head of bacteriophage T4. *Nature* **227**, 680-685.

Letwin, K., Mizzen, L., Motro, B., Ben-David, Y., Bernstein, A. and Pawson, T. (1992). A mammalian dual specificity protein kinase, Nek1, is related to the NIMA cell cycle regulator and highly expressed in meiotic germ cells. *EMBO J.* **11**, 3521-3531.

Liu, S., Lu, W., Obara, T., Kuida, S., Lehoczky, J., Dewar, K., Drummond, I. A. and Beier, D. R. (2002). A defect in a novel Nek-family kinase causes cystic kidney disease in the mouse and in zebrafish. *Development* **129**, 5839-5846.

Mahjoub, M. R., Montpetit, B., Zhao, L., Finst, R. J., Goh, B., Kim, A. C. and Quarmby, L. M. (2002). The FA2 gene of Chlamydomonas encodes a NIMA family kinase with roles in cell cycle progression and microtubule severing during deflagellation. *J. Cell Sci.* **115**, 1759-1768.

Mahjoub, M. R., Qasim Rasi, M. and Quarmby, L. M. (2004). A NIMA-related kinase, Fa2p, localizes to a novel site in the proximal cilia of Chlamydomonas and mouse kidney cells. *Mol. Biol. Cell* **15**, 5172-5186.

Marshall, W. F. and Rosenbaum, J. L. (2000). How centrioles work: lessons from green yeast. *Curr. Opin. Cell Biol.* **12**, 119-125.

O'Connell, M. J., Krien, M. J. and Hunter, T. (2003). Never say never. The NIMA-related protein kinases in mitotic control. *Trends Cell Biol.* **13**, 221-228.

Ogbadoyi, E., Ersfeld, K., Robinson, D., Sherwin, T. and Gull, K. (2000). Architecture of the *Trypanosoma brucei* nucleus during interphase and mitosis. *Chromosoma* **108**, 501-513.

Ogbadoyi, E. O., Robinson, D. R. and Gull, K. (2003). A high-order trans-membrane structural linkage is responsible for mitochondrial genome positioning and segregation by flagellar basal bodies in trypanosomes. *Mol. Biol. Cell* **14**, 1769-1779.

Parsons, M., Worthey, E. A., Ward, P. N. and Mottram, J. C. (2005). Comparative analysis of the kinomes of three pathogenic trypanosomatids: Leishmania major, Trypanosoma brucei and Trypanosoma cruzi. *BMC Genomics* **6**, 127.

Ploubidou, A., Robinson, D. R., Docherty, R. C., Ogbadoyi, E. O. and Gull, K. (1999). Evidence for novel cell cycle checkpoints in trypanosomes: kinetoplast segregation and cytokinesis in the absence of mitosis. *J. Cell Sci.* **112**, 4641-4650.

Polci, R., Peng, A., Chen, P. L., Riley, D. J. and Chen, Y. (2004). NIMA-related protein kinase 1 is involved early in the ionizing radiation-induced DNA damage response. *Cancer Res.* **64**, 8800-8803.

Rechsteiner, M. and Rogers, S. W. (1996). PEST sequences and regulation by proteolysis. *Trends Biochem. Sci.* **21**, 267-271.

Rhee, K. and Wolgemuth, D. J. (1997). The NIMA-related kinase **2**, Nek2, is expressed in specific stages of the meiotic cell cycle and associates with meiotic chromosomes. *Development* **124**, 2167-2177.

Robinson, D. R. and Gull, K. (1991). Basal body movements as a mechanism for mitochondrial genome segregation in the trypanosome cell cycle. *Nature* **352**, 731-733.

Robinson, D. R., Sherwin, T., Ploubidou, A., Byard, E. H. and Gull, K. (1995). Microtubule polarity and dynamics in the control of organelle positioning, segregation, and cytokinesis in the trypanosome cell cycle. *J. Cell Biol.* **128**, 1163-1172.

Sherwin, T. and Gull, K. (1989). The cell division cycle of *Trypanosoma brucei brucei*: timing of event markers and cytoskeletal modulations. *Philos. Trans. R. Soc. Lond. B Biol. Sci.* **323**, 573-588.

Spurr, A. R. (1969). A low-viscosity epoxy resin embedding medium for electron microscopy. *J. Ultrastruct. Res.* **26**, 31-43.

Tu, X. and Wang, C. C. (2004). The involvement of two cdc2-related kinases (CRKs) in Trypanosoma brucei cell cycle regulation and the distinctive stage-specific phenotypes caused by CRK3 depletion. *J. Biol. Chem.* **279**, 20519-20528.

Twomey, C., Wattam, S. L., Pillai, M. R., Rapley, J., Baxter, J. E. and Fry, A. M. (2004). Nek2B stimulates zygotic centrosome assembly in *Xenopus laevis* in a kinase-independent manner. *Dev. Biol.* **265**, 384-398.

Upadhya, P., Birkenmeier, E. H., Birkenmeier, C. S. and Barker, J. E. (2000). Mutations in a NIMA-related kinase gene, Nek1, cause pleiotropic effects including a progressive polycystic kidney disease in mice. *Proc. Natl. Acad. Sci. USA* **97**, 217-221.

Vickerman, K. (1985). Developmental cycles and biology of pathogenic trypanosomes. *Br. Med. Bull.* **41**, 105-114.

Vickerman, K., Tetley, L., Hendry, K. A. and Turner, C. M. (1988). Biology of African trypanosomes in the tsetse fly. *Biol. Cell* **64**, 109-119.

Westermann, S. and Weber, K. (2002). Identification of CfNek, a novel member of the NIMA family of cell cycle regulators, as a polypeptide copurifying with tubulin polyglutamylation activity in Crithidia. *J. Cell Sci.* **115**, 5003-5012.

Wirtz, E., Leal, S., Ochatt, C. and Cross, G. A. (1999). A tightly regulated inducible expression system for conditional gene knock-outs and dominant-negative genetics in *Trypanosoma brucei*. *Mol. Biochem. Parasitol.* **99**, 89-101.

Journal of Cell Science